J Biol Inorg Chem (2005) 10: 831–841
DOI 10.1007/s00775-005-0031-3

ORIGINAL ARTICLE

T. Fujimori · S. Yamada · H. Yasui · H. Sakurai
Y. In · T. Ishida

Orally active antioxidative copper(II) aspirinate: synthesis, structure characterization, superoxide scavenging activity, and in vitro and in vivo antioxidative evaluations

Received: 13 May 2005 / Accepted: 9 September 2005 / Published online: 28 October 2005

Abstract Ever since it was proposed that reactive oxygen species (ROS) are involved in the pathogeneses of various diseases, superoxide dismutase (SOD)-mimetic complexes have been intensively studied. We prepared copper(II) aspirinate [$Cu_2(asp)_4$] from Cu(II) and aspirin, which has been in use for many years as an antipyretic, an analgesic, and an anti-inflammatory agent. However, $Cu_2(asp)_4$ has been found to have additional activities, including anti-inflammatory, antiulcer, anti-ischemic/reperfusion agent, anticancer, antimutagenic, and antimicrobial activities. The activity of copper salicylate [$Cu(sal)_2$] was also compared with that of $Cu_2(asp)_4$. The structure of the $Cu_2(asp)_4$ was determined using X-ray structure analysis. Its SOD-mimetic activity was determined usingcytochrome c, electron spin resonance (ESR) spectroscopy, and ESR spin trap methods. The activity of $Cu_2(asp)_4$ was slightly greater than $CuSO_4$ and copper acetate [$Cu(ace)_2$] and slightly less than that of $Cu(sal)_2$. The in vitro antioxidant activity, evaluated in human epithelial or transformed neoplastic keratinocyte cells, HaCaT, and normal dermal fibroblasts in terms of cell survival following ultraviolet B (UVB) irradiation, was significantly increased in the presence of $Cu_2(asp)_4$, $Cu(sal)_2$, and $CuSO_4$. Further, ROS generation following UVA irradiation in the skin of hairless mice following oral treatment with $Cu_2(asp)_4$ for three consecutive days was significantly suppressed compared to the vehicle- or $Cu(ace)_2$-treated mice. On the basis of these results, $Cu_2(asp)_4$ was observed to be a potent antioxidative compound possessing antioxidative activity in biological systems. In conclusion, $Cu_2(asp)_4$ is a potent antioxidative agent that may be useful for future treatment of diseases resulting from ROS.

Keywords Copper aspirinate · Copper salicylate · Copper acetate · Copper sulfate · HaCaT cell · Fibroblasts · Reactive oxygen species · Skin

T. Fujimori · S. Yamada · H. Yasui · H. Sakurai (✉)
Department of Analytical and Bioinorganic Chemistry,
Kyoto Pharmaceutical University, 5 Nacauchi-cho,
Misasagi, Yamashina-ku, Kyoto 607-8414, Japan
E-mail: sakurai@mb.kyoto-phu.ac.jp
Tel.: +81-75-5954629
Fax: +81-75-5954753

Y. In · T. Ishida
Department of Physical Chemistry,
Osaka University of Pharmaceutical Sciences,
4-20-1 Nasahara, Takatsuki, Osaka 569-1094, Japan

Introduction

It has been proposed that reactive oxygen species (ROS) are involved in the pathogeneses of various diseases, such as lifestyle-related diseases including hypertension [1] and photoaging due to exposure to ultraviolet radiation. Cu-dependent and Zn-modulated cytosolic and extracellular superoxide dismutases (Cu_2Zn_2SOD), which are present in a wide range of animals (including man), catalyze the dismutation reaction of superoxide ($\cdot O_2^-$) to yield hydrogen peroxide (H_2O_2) and triplet state oxygen ($^3O_2$) [2]. SOD activity in mammalian cells, including those of man, tends to decrease with age; hence, the intake of SOD-enhancing compounds capable of facilitating de novo synthesis of Cu_2Zn_2SOD is recommended [3]. Since SOD is labile to gastric and intestinal proteases, which cause digestion of this enzyme, oral intake of small-molecular-mass SOD-mimetic complexes with similar Cu_2Zn_2SOD active site structures was originally proposed by Sorenson [4] and then intensively developed by many researchers [5–11].

During our study of the development of SOD-mimetic metalloelement complexes [12–14], we planned the preparation of Cu(II) complexes with pharmacologically active ligands. It is well known that Cu(II) has superoxide scavenging activity and that aspirin has been used for many years as an antipyretic, an analgesic, and an anti-inflammatory agent; in recent years it has also been used as a platelet anti-aggregating agent [15, 16], an antitumor agent [17], and as a protective agent against UV exposure [18, 19]. Subsequently, we prepared

copper(II) aspirinate [$Cu_2(asp)_4$] for evaluation as a SOD-mimetic with an active center similar to the active center of Cu_2Zn_2SOD [20] in order to achieve a synergistic effect for the combination of Cu(II) and aspirin and to compare its activity with copper salicylate [$Cu(sal)_2$].

Previously, it was reported that the three-dimensional X-ray crystal structure of $Cu_2(asp)_4$ was binuclear [21], that it exhibited anti-inflammatory activity in rats at a dose of 10 μmol/kg of body mass, while the lowest active dose of aspirin was 360 μmol/kg [8], and that $Cu_2(asp)_4$ was less irritating to the gastric mucosa and had anti-ulcer activity [8]. These results strongly indicated that $Cu_2(asp)_4$ was useful for the treatment of ROS-related disorders and diseases. Thus, our aim was to comprehensively examine this complex in terms of its ROS suppressive effects.

We also determined: (1) the X-ray crystal structure of a derivative of $Cu_2(asp)_4$, $Cu_2(asp)_4(DMSO)_2$; (2) the SOD-mimetic activities of $Cu_2(asp)_4$ and $Cu(sal)_2$ using the xanthine–xanthine oxidase–cytochrome c enzyme system, direct ESR spectrometry, and the ESR spin trap method; (3) their in vitro antioxidative activities in both an immortalized human epithelial or transformed keratinocyte cell line, HaCaT, and a normal human dermal fibroblast cell line (NHDF), using a UVB irradiation model to measure the relative cell survival; (4) the suppressive effects of an orally administered 5% aqueous acacia suspension of $Cu_2(asp)_4$ and $Cu(sal)_2$ on UVA-induced ROS generation of hairless mouse skin; and finally (5) the concentration of Cu in the blood and skin of ICR mice treated with Cu(II) compounds or ligands. Based upon these results, it is proposed that $Cu_2(asp)_4$ and $Cu(sal)_2$ are potent orally active antioxidative agents.

Materials and methods

Aspirin (acetylsalicylic acid), cytochrome c, Cu_2Zn_2 superoxide dismutase (Cu_2Zn_2SOD) and neutral red were purchased from Sigma. Xanthine sodium salt was obtained from Nacalai Tesque (Kyoto, Japan). Copper(II) sulfate pentahydrate, salicylic acid, xanthine oxidase isolated from butter milk (XOD), dimethyl sulfoxide (DMSO), *N*, *N*-dimethylformamide (DMF), diethylenetriamine-*N*, *N*, *N*′, *N*″, *N*″-pentaacetic acid (DTPA), nitric acid, perchloric acid, and hydrogen peroxide were purchased from Wako Pure Chemicals (Osaka, Japan). 2,2,6,6-Tetramethyl-4-piperidone (TMPD), potassium superoxide (KO_2) and dibenzo-18-crown-6 (DB18C6) were purchased from Aldrich. Dulbecco's modified Eagle's medium (DMEM) was purchased from Nikken Biomedical Laboratory (Kyoto, Japan). Fetal bovine serum (FBS) was purchased from Equitech Bio (Ingram, TX, USA). 5,5-Dimethyl-1-pyrroline-*N*-oxide (DMPO) was purchased from Labotec (Tokyo, Japan) and 2-methyl-6-phenyl-3,7-dihydroimidazo(1,2-a)pyrazin-3-one (CLA) was purchased from Tokyo Kasei (Kogyo, Tokyo, Japan).

Animals and cells

Male HR-1 hairless mice (five weeks old) and ICR mice (five weeks old) were purchased from Shimizu Experimental Materials (Kyoto, Japan) and were maintained in facilities with a 12 h light/dark cycle at the central animal facility of the Kyoto Pharmaceutical University (KPU) for experimental periods. These animals were given free access to standard mouse chow and water during these periods. The HaCaT cells, an immortalized human epithelial or transformed neoplastic keratinocyte cell line, were kindly provided by Dr. Masaki. Normal human dermal fibroblasts from neonatal foreskin (NHDF) were purchased from Kurabo Biomedical Business (Osaka, Japan).

Syntheses

Preparation of $Cu_2(asp)_4$

The $Cu_2(asp)_4$ complex was prepared as previously reported [20]. In brief, aspirin (3.60 g, 0.02 mol) was allowed to dissolve in a solution of potassium bicarbonate (2.01 g, 0.02 mol) in 30 ml of water. A solution of copper(II) sulfate pentahydrate (2.50 g, 0.01 mol) in 20 ml of water was slowly added to the above-mentioned solution with constant stirring. An aquamarine precipitate formed and the pH of the solution fell from 6.1 to 4.8. The precipitate was collected in a sintered glass funnel, washed with deionized water, and dried in the funnel attached to laboratory vacuum. This compound had a 255 °C decomposition point. Elemental analysis data are presented in Table 1.

Crystals of a DMSO adduct of $Cu_2(asp)_4$, $Cu_2(asp)_4(DMSO)_2$, suitable for X-ray crystal structure analysis, were prepared by dissolving 0.015 mmol of $Cu_2(asp)_4$ in 10 ml of DMSO at room temperature and allowed to stand at room temperature for over one - month.

Preparation of $Cu(sal)_2$

The $Cu(sal)_2$ complex was prepared as reported [20, 22]. In brief, salicylic acid (2.76 g, 0.02 mol) was dissolved in a solution of potassium bicarbonate (2.01 g, 0.02 mol) in 30 ml of water with heating at 35 °C. A solution of copper(II) sulfate pentahydrate (2.50 g, 0.01 mol) in 20 ml of water was slowly added to the above-mentioned solution with constant stirring under heating at 35 °C. A green-yellow precipitate formed and the pH ranged from 3.5 to 6.0. The precipitate was collected by filtration using a sintered glass funnel, washed with deionized water, and dried in a funnel attached to laboratory vacuum. This complex decomposed on heating to 158 °C. Elemental analytical data are presented in Table 1.

Table 1 Physicochemical properties of Cu(II) complexes

ESR parameters				
Complex	Solvent	$g_{\perp}$	g_{II}	A_{II} (10^{-4} cm^{-1})
$Cu_2(asp)_4$	DMSO	2.07	2.36	137
$Cu(sal)_2$	DMSO	2.07	2.37	151

		Element analysis		Visible absorption spectrum λ_{max} (nm)		
		H(%)	C (%)	DMSO	DMF	Solid state
$Cu_2(asp)_4$	calcd.	3.39	50.93	748	722	662
$C_{36}H_{28}Cu_2O_{16}(H_2O)_{0.3}$ [843.7]	found	3.40	50.99			
$Cu(sal)_2$	calcd.	3.57	46.23	416 784	745	693
$C_{14}H_{10}CuO_6(H_2O)_{1.4}$ [337.8]	found	3.39	46.23			

	IR spectrum		Magnetic susceptibility[a]
	$\nu_{Cu-O}(cm^{-1})$	$\nu_{C=O}(cm^{-1})$	$\mu_{eff}^{(24\ °C)}$
$Cu_2(asp)_4$	502	1,726 (1,692 aspirin)	2.04
$Cu(sal)_2$	590	1,659 (1,654 salicylic acid)	1.77

[a]Theoretical $\mu_{eff} = 1.8 \sim 2.1$

Determination of physicochemical properties of the complexes

The IR spectra were obtained using the KBr disc method with a FTIR-8100A spectrophotometer (Shimazu, Japan). The ESR spectra were obtained with an X-band ESR spectrometer RE-1X (Joel Ltd., Tokyo, Japan). The visible absorption spectra were obtained using a DMSO solution and a KBr disc with an Agilent spectrophotometer (Yokogawa Analytical Systems, Tokyo, Japan) and MCPD-1000 spectrophotometer (Otsuka Electronics, Osaka, Japan), respectively. Magnetic susceptibilities were obtained with a magnetic susceptibility balance (MK I, Sherwood Scientific, Cambridge, England).

X-ray structure determination of $Cu_2(asp)_4$

A single crystal with dimensions 0.4×0.2×0.20 mm^3 was used for X-ray crystallography. The X-ray data were collected with a Bruker (Karlsruhe, Germany) SMART APEX CCD camera using graphite-monochromated MoK ($\lambda = 0.71073$ Å) at 120 K. The structure was solved by a direct method using the SHELXS97 program [23]. Atomic scattering factors were taken from international tables for X-ray crystallography [24]. The positional parameters of non-H atoms were refined by a full matrix least squares method with anisotropic thermal parameters using the program SHELXL97 [25].

Assay of superoxide scavenging activity (SSA)

Xanthine/xanthine oxidase/cytochrome c method

The reduction of cytochrome c (λ_{max}, 550 nm) in a xanthine–xanthine oxidase system was measured at 550 nm using a Ubest-55 UV–VIS spectrometer (Jasco, Tokyo, Japan) in the presence of different amounts of Cu(II) complexes dissolved in DMSO and $CuSO_4$ in deionized water. The increase (ΔA_{550}) in the absorbance was monitored 45 s after the initiation of the reaction for 90 s. The SSA of a compound was expressed as an IC_{50} value, which defines 50% of the inhibitory concentration of a compound in the reaction [26].

Direct ESR spectroscopic method for the measurement of SSA

Both 3.17 mg (0.045 mmol) of KO_2 and 27.8 mg (0.077 mmol) of DB18C6 were combined in a test tube with 5 ml of a mixture of toluene and DMSO (3:2 v/v). The resultant solution was purged with argon gas for 60 s and sealed with a septum and then sonicated for 2 min. The supernatant was used for ESR measurements. One hundred microliters of different concentrations of the test compounds in DMF (ranging from 0 to 10 μM) was added to 200 μL of the KO_2 and DB18C6 toluene/DMSO solution in a $\phi = 5$ mm quartz ESR cell. After mixing, the solution was frozen at liquid nitrogen temperature and the resultant ESR spectrum was recorded using an X-band ESR spectrometer RE-1X (JOEL) [27].

ESR spin trap method using DMPO

Superoxide Superoxide formed in a hypoxanthine–xanthine oxidase–DMPO system composed of 2.8 mM of hypoxanthine, 1 U/mL of xanthine oxidase, 0.125 mM DTPA, and 2.25 M DMPO was trapped by DMPO and the ESR spectrum recorded at room temperature (22 °C) using an X-band ESR spectrometer

JES-RFR30 (JOEL). The ratio of the signal intensity (S) appearing at the lowest magnetic field due to the DMPO–OO(H) adduct to that of the third signal intensity (M) due to Mn(II) was termed the S/M ratio. The SSA of the Cu(II) compound added in DMSO or water ranging in concentration from 0 to 20 μM was determined based upon the IC_{50} value, which defines the 50% inhibitory concentration of the compound showing the 50% S/M ratio to vehicle control [28].

Singlet oxygen Singlet oxygen formed in a hematoporphyrin (0.25 mM phosphate buffer, pH 7.4) irradiated with UVA light (through a UVA filter at a dose of 800 mW cm^{-2} using a Superure-203S, San-Ei Electric MFG, Japan) was trapped with 200 mM TMPD and its ESR spectrum was recorded using an X-band ESR spectrometer JES-RFR30 (JOEL) in a manner similar to that employed for superoxide trapping, using 0–150 μM Cu(II) compounds added in DMSO or water [28].

Cell cultures and UVB irradiation

Cells, maintained in DMEM supplemented with 5% FBS, were grown in a humidified incubator at 37 °C with 5% CO_2 atmosphere. HaCaT and fibroblast cells were placed in a 96-well microplate at densities of 3×10^4 or 2×10^4 cells per well, respectively. After 24 hours of cultivation, the medium was replaced with DMEM containing different concentrations of the test compounds dissolved in DMSO or water ranging from 0 to 15 μM. The final concentration of DMSO in each test solution was 0.5%. After 24 hours of cultivation, these media were replaced with Hanks' balanced salt solution and exposed to UVB irradiation using a FL20SE lamp (Toshiba Medical Supply, Tokyo, Japan) as a radiation source. UVB irradiation was performed with intensities of 60 mJ cm^{-2} or 300 mJ cm^{-2} for HaCaT cells or fibroblast cells, respectively. After UVB irradiation, these cells were placed in DMEM supplemented with 5% FBS and cultured for 24 h at 37 °C. Cell survival was determined using the neutral red method. Neutral red incorporated into the cells was solubilized with 100 μL of 30% EtOH in 0.1 M HCl and its absorbance was measured at 560 nm with reference to the absorbance at 660 nm using a plate reader TECAN SPECTRAFluor Plus (TECAN, Hombrechtikon, Switzerland). Survival was expressed as a percentage of the amount of neutral red incorporated into sham UVB irradiated cells [29–31].

In vivo chemiluminescent measurement in hairless mice

Compounds were suspended in 5% acacia–deionized water solution and doses of 240 μmol $Cu_2(asp)_4$ kg^{-1}, 480 μmol $Cu(sal)_2$ kg^{-1}, 480 μmol $Cu(ace)_2$ kg^{-1}, 960 μmol aspirin kg^{-1} or 960 μmol salicylic acid kg^{-1} were administered orally for three consecutive days to six-week-old male hairless mice (HR-1). These mice were anesthetized by intraperitoneal injection of 50 mg pentobarbital kg^{-1} body mass and placed on a heating pad for 30 min after last treatment. The skin surfaces of these mice were carefully cleaned with aqueous 50% ethanol and each mouse was covered with a black cloth in which two holes were cut. The holes on the right sides of the mice were irradiated with 18 J cm^{-2} UVA, while the left side was unexposed; subsequently, 200 μM CLA (10 μL) was applied to the measurement areas of the skin of the mouse. Chemiluminescence emitted from a single given area (78.5 mm^2) in the skin below the hole was measured for 30 m with a supersensitive chemiluminescence-measuring apparatus, a NightOWL (luminograph LB 981, Wallack Berthold, Germany), which provides chemiluminescent (CL) intensity (photons/pixel/second) as well as CL imaging. The area under the curve (AUC) of measured CL intensities vs time was evaluated (mega photons/pixel) [32, 33].

Measurement of Cu concentration

Compounds were suspended in 5% acacia–deionized water solution and each compound at doses of 240 μmol $Cu_2(asp)_4$ kg^{-1}, 480 μmol $Cu(sal)_2$ kg^{-1}, 480 μmol $Cu(ace)_2$ kg^{-1}, 960 μmol aspirin kg^{-1} or 960 μmol salicylic acid kg^{-1} was administered orally for three consecutive days to six-week-old ICR mice. Blood was drawn from vena cave 30 or 90 m after the last treatment on day 3. The skin was removed from the abdomen of each mouse 90 min the after last treatment on day 3, prior to removing the skin, and the hair on the abdomen of each mouse was shaved with an electric clipper on day 2. The samples were stored frozen at −80 °C until metal analysis was performed by atomic absorption spectrophotometry (AA-6300, Shimazu, Japan). Fifty microliters of each blood sample and approximately 40 mg of each skin sample were analyzed after ashing in concentrated nitric acid/perchloric acid/hydrogen peroxide.

All mouse experiments were approved by the Experimental Animal Research Committee of KPU and conducted according to the KPU guidelines for Animal Experimentation.

Statistical analyses

All experimental results are expressed as the mean ± standard deviation (SD) of triplicate determinations. Statistical analysis was performed by analysis of variance (ANOVA) at a 1% or 5% significance level of difference.

Results

Physicochemical properties and X-ray crystal structure of $Cu_2(asp)_4$

Physicochemical properties

The physicochemical properties of successfully synthesized $Cu_2(asp)_4$ and $Cu(sal)_2$ were established via elemental analysis, ESR spectra, IR spectra, liquid and solid state visible absorption spectra, and magnetic susceptibility. These results are listed in Table 1. The physicochemical properties of these complexes agreed well with previously reported data [20, 22, 34]. Elemental analyses suggested 2:1 ligand to Cu(II) complex formation. The strong IR shift of the carboxylate group in both complexes compared with that of each ligand [aspirin $\nu_{C=O}$ for carboxylate at 1,692 cm^{-1} versus $Cu_2(asp)_4$ $\nu_{C=O}$ for carboxylate at 1,726 cm^{-1} and salicylic acid $\nu_{C=O}$ for carboxylate at 1,657 cm^{-1} vs. $Cu(sal)_2$ $\nu_{C=O}$ for carboxylate at 1,659 cm^{-1}] indicate coordinate bonding of carboxylate groups with Cu(II). Magnetic susceptibility indicated the presence of Cu(II) in these complexes. The ESR spectra for these complexes demonstrate the existence of mononuclear complexes in the polar DMSO solvent (Fig. 1) and that these complexes possessed the CuO_4 coordinate structure in DMSO solution based upon the ESR parameters $g_{\|}$ and $A_{\|}$, in which four oxygen molecules are coordinately bonded to a Cu(II) center [35].

X-ray crystal structure

Crystal data, experimental conditions, and results from X-ray crystallographic studies of $Cu_2(asp)_4(DMSO)_2$ are listed in Table. 2 and 3. The oxygen atoms of two DMSO solvate molecules were found to be axially bonded to the Cu(II) atoms. The positions of the H atoms were all calculated on the basis of their stereochemical requirements. These H atoms were treated as riding with fixed isotropic displacement parameters, $U_{iso} = 1.2 \times U_{eq}$, for the associated C or N atoms or $U_{iso} = 1.5 \times U_{eq}$ for the methyl C or O atoms; their atomic positions were not included as variables for the refinements. None of the positional parameters for non-H atoms shifted more than their estimated standard deviations, and the residual electron density in the final difference Fourier map was in the range of –0.909 to 0.134 $e/Å^{-3}$. The final atomic coordinates, anisotropic temperature factors, bond lengths, bond angles, torsion angles of non-H atoms, and the atomic coordinates of H atoms have been deposited at the Cambridge Crystallographic Data Center (CCDC 256313) (Cambridge University Chemical Laboratory, Cambridge, UK).

X-ray structure analysis of $Cu_2(asp)_4(DMSO)_2$ shows that the crystal structure is constructed from binuclear units, as shown in Fig. 2 for $Cu_2(asp)_4(DMSO)_2$, and each half of the binuclear unit is related to the other by a crystallographic center of symmetry. Four aspirin molecules are bonded to the two copper atoms through four carboxylate bridges to form a single $Cu_2(CO_2)_4$ unit. The copper atoms and eight carboxylate oxygen atoms of aspirin form an octahedron with equatorial bonding and axial bonding of the two DMSO molecules to the copper atoms.

SSA of Cu(II) compounds

Three methods of SSA assay; the xanthine/xanthine oxidase/cytochrome c method, direct ESR spectroscopy, and an ESR spin trap method were used to measure the scavenging activities of the copper compounds examined. The concentrations of these compounds needed to cause 50% removal of superoxide were determined as IC_{50} values, as listed in Table 4. SOD-mimetic activities were almost equivalent for the two Cu(II) complexes, $Cu_2(asp)_4$ and $Cu(sal)_2$, as well as for $CuSO_4$, which was approximately one-six hundredth of the activity of Cu_2Zn_2SOD determined using the xanthine/xanthine oxidase/cytochrome *c* method. No activity was observed for the ligands (aspirin and salicylic acid). Since the generated $\cdot O_2^-$ (Fig. 3) was scavenged by all Cu(II) compounds, this reactivity is attributed to the direct reaction of Cu(II) with $\cdot O_2^-$. Singlet oxygen scavenging activity was not observed for these Cu(II) compounds in the range of 0–150 μM based on results obtained with the ESR spin trap method (data is not shown).

Suppression of UVB irradiation-induced cell damage by $Cu_2(asp)_4$, $Cu(sal)_2$, and $CuSO_4$

The UVB irradiation dose was fixed at 60 mJ cm^{-2}, which corresponded to the radiation dose that would allow 60% cell survival as compared to 100% survival for unirradiated HaCaT cells. In contrast to the 60% survival of irradiated HaCaT cells grown in medium containing no Cu(II) compound addition, addition of $Cu_2(asp)_4$, $Cu_2(sal)_4$ and $CuSO_4$ dissolved in DMSO enhanced cell survival in a dose-dependent manner in the concentration range 0–15 μM based on Cu concentration (Fig. 4). Further, these three compounds exhibited cell survival enhancing abilities, with the following magnitudes: $Cu(sal)_2 > Cu_2(asp)_4 > CuSO_4$. Slight and insignificant increases in cell survival were observed with the addition of aspirin or salicylic acid.

For fibroblast cells, the UVB irradiation dose was fixed at 300 mJ cm^{-2}, which also gave 60% cell survival following UVB irradiation as compared to survival without UVB irradiation. Fibroblasts were more sensitive to the Cu(II) compounds than HaCaT cells. Addition of Cu complexes or $CuSO_4$ dissolved in DMSO enhanced cell survival in a dose-dependent manner over the concentration range 0–3.8 μM based

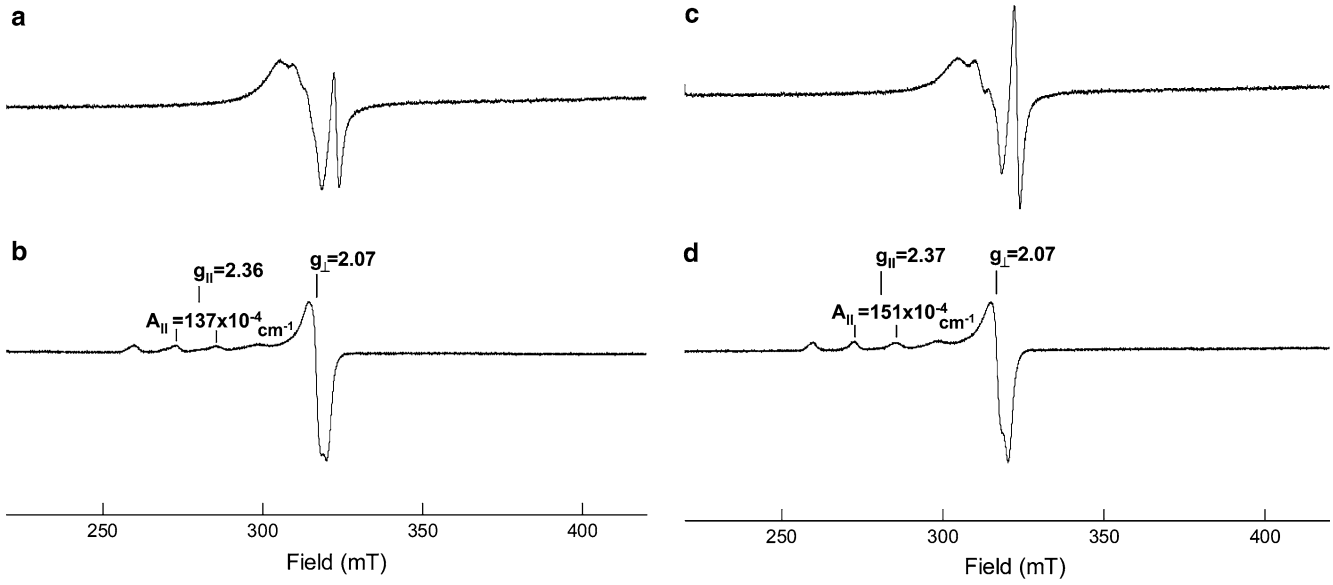

Fig. 1a–d ESR spectra of $Cu_2(asp)_4$ at room temperature (**a**), at 77 K (**b**); $Cu(sal)_2$ at room temperature (**c**); and $Cu(sal)_2$ at 77 K (**d**), dissolved in DMSO

Table 2 Conditions used for the determination of $Cu_2(asp)_4(DMSO)_2$

Eλmpirical formula	$Cu(C_9H_7O_4)_2(C_2H_6SO)_2$	*Z* value	2
Formula weight	578.09	ρ/g cm^{-3}	1.483
Crystal dimensions/mm^3	0.4×0.2×0.20 mm^3	*F*(000)	598
Crystal system	Triclinic	m(Mo Kα)/cm^{-1}	1.057
Lattice parameters		Temperature/K	288
a/Å	9.724(2)	λ/Å	0.71073
b/Å	12.193(2)	θ_{max}/°	28.26
c/Å	12.692(2)	No. of observation	5709
α/°	110.255(3)	No. of variables	338
β/°	105.536(3)		
γ/°	100.652(3)	;*w R*	0.069; 0.206
V/Å^3	1294.5(4)	GOF	1.052
Space group	*P*1		

on Cu concentrations; however, doses above 15 μM caused cell toxicity (Fig. 5). The order of cell survival was: $Cu(sal)_2$ > $Cu_2(asp)_4$ > $CuSO_4$.

Suppression of reactive oxygen species generated with UVA irradiation of hairless mouse skin with $Cu_2(asp)_4$

The UVA-induced generation of ROS (evidenced by chemiluminescence intensity) following UVA-irradiation of hairless mouse skin treated with $Cu_2(asp)_4$ or $Cu(sal)_2$ orally for three consecutive days was significantly suppressed as compared with vehicle-treated control and $Cu(ace)_2$-, aspirin-, or salicylic acid-treated mice (Fig. 6). It is noteworthy that the administration of $Cu(ace)_2$, which was less toxic than $CuSO_4$, exhibited no inhibition of ROS generation in the skin of each mouse. These results show that $Cu_2(asp)_4$ had a greater in vivo ROS suppressing effect than the other copper(II) compounds (Table 5).

Table 3 $Cu_2(asp)_4$ with DMSO or DMF axial ligands

Complex	Cu–Cu (Å)	Cu–O (basal) (Å)	Cu–O (axial) (Å)	O–C (carboxylate) (Å)	Cu–basal plane (Å)	Cu–O–C (°)	O–C–O (°)	Reference
$[Cu_2(asp)_4(DMSO)_2]$	2.632(1)	1.963(3)	2.131(3)	1.258(6)	0.1963(3)	122.8(2)	125.8(4)	
$[Cu_2(asp)_4(DMF)_2]$	2.6154(4)	1.9533(12)	2.1540(12)	1.256(2)	0.187	119.92(11)	125.69(15)	[14]
		1.9711(11)		1.268(2)		125.15(11)	125.76(15)	
$[Cu_2(asp)_4]$	2.617(3)	1.963(4)	2.241(8)	1.26(1)	0.190	120.7(7)	125(1)	[29]
						125.9(8)	126(1)	

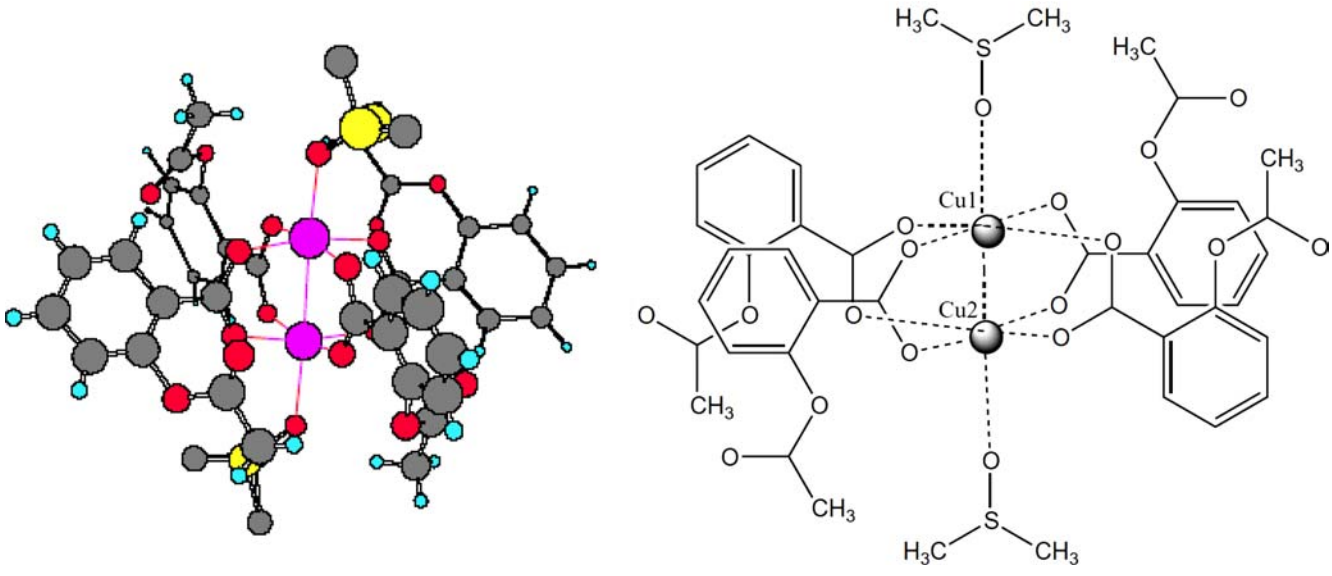

Fig. 2 The structure of $Cu_2(asp)_4(DMSO)_2$

Cu concentration in the blood and skin of ICR mice treated with Cu compounds or ligands

The distribution of Cu in ICR mice treated with Cu(II) compounds and ligands orally for three consecutive days was determined by AAS. The blood Cu concentrations 30 and 90 min after the last administration of the compounds on day 3 and the skin Cu concentrations 90 min after the last administration are shown in Table 6. The Cu concentration of the $Cu(ace)_2$ group was increased 30 min after the last administration, although the Cu concentration of the $Cu(ace)_2$ group was normal 90 min after the administration. On the other hand, the Cu concentrations of the $Cu_2(asp)_4$ and $Cu(sal)_2$ groups were slightly increased 90 min after administration. The Cu concentration in the skin treated with $Cu_2(asp)_4$ was slightly increased.

Discussion

The X-ray structure analysis of $Cu_2(asp)_4(DMSO)_2$ indicates that its crystal structure is binuclear with a crystallographic center of symmetry (Fig. 2). Four aspirin molecules are bonded to two Cu(II) atoms through four carboxylate bridges to form a $Cu_2(CO_2)_4$ unit. Each Cu(II) atom forms a hemi-octahedral coordinated moiety with the equatorial positions occupied by four carboxylate oxygens of two aspirin molecules, and with the axial positions occupied by the oxygen atom of DMSO. The crystal structure of $Cu_2(asp)_4$ [21] and the DMF solvate, $Cu_2(asp)_4(DMF)_2$ [36], have been previously reported [21]. In the present study, we analyzed the crystal structure of the DMSO solvate (Table 2). The axial coordination positions of the Cu(II) atoms in

Table 4 Superoxide scavenging activity (SSA) of Cu(II) compounds

Compound	IC_{50} (μM) (mean ± s.d.) *		
	cytochrome c	direct ESR	ESR spin trap
$Cu_2(asp)_4$	1.83 ± 0.12	0.63 ± 0.01	12.8 ± 0.52
$Cu(sal)_2$	1.23 ± 0.04	0.65 ± 0.11	13.5 ± 0.35
$CuSO_4$	1.79 ± 0.03	0.79 ± 0.13	12.9 ± 0.38
$Cu(ace)_2$	1.71 ± 0.08		
Cu_2Zn_2SOD	2.65 ± 0.07 nM		

** $P < 0.01$

* Data are represented as means ± standard derivation (n=3) based on Cu concentration.

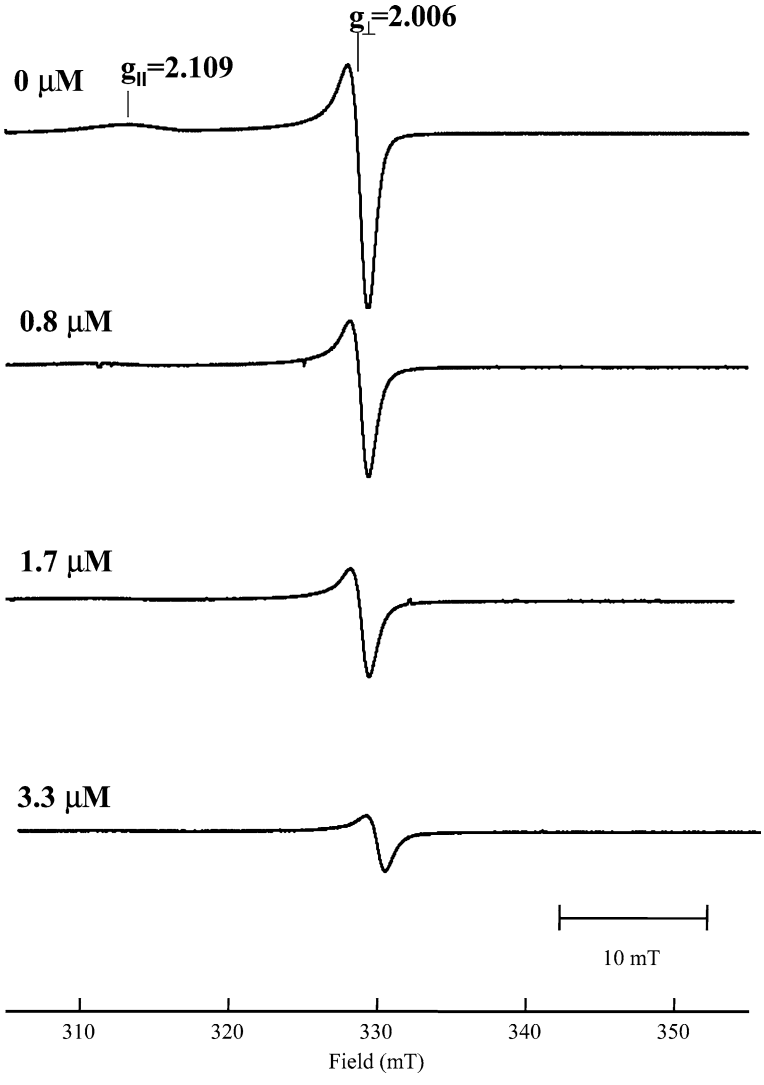

Fig. 3 Superoxide scavenging activity of $Cu_2(asp)_4$ as determined with ESR at 77 K. The indicated concentrations in toluene and DMSO solutions are based on Cu concentrations

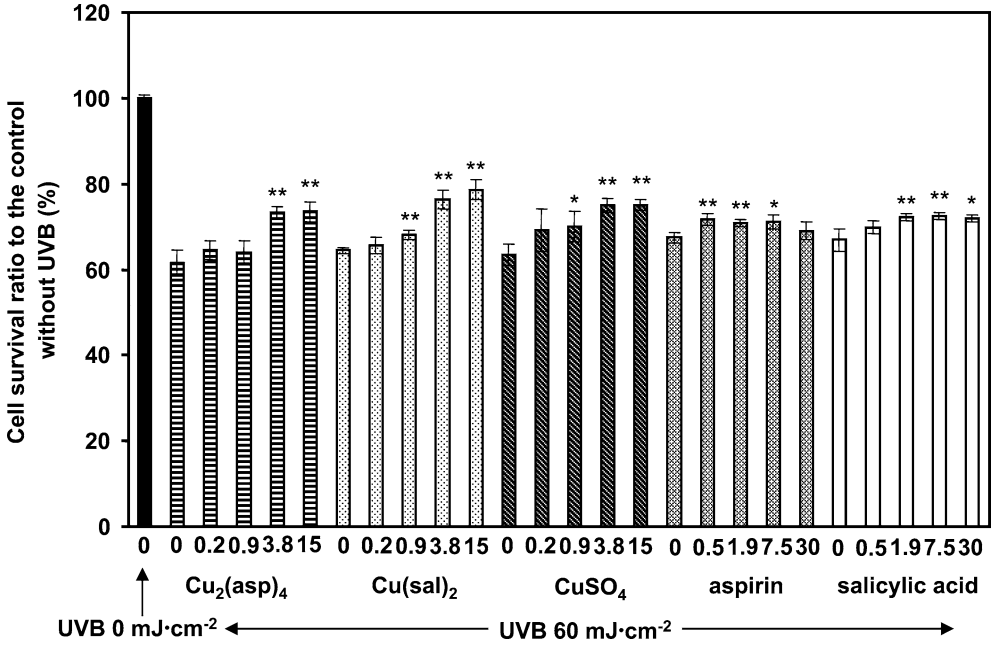

Fig. 4 Effects of $Cu_2(asp)_4$ and its related compounds (in DMSO) on the survival of HaCaT cells. Units of concentration are micrometers. The *left column* of each panel shows the control result without UVB irradiation. The other columns list results obtained for cells treated with complexes and UVB-irradiated. The indicated concentrations are based on Cu content. Data are expressed as the mean ± SD for three replicate determinations. $^{**}P < 0.01$, $^{*}P < 0.05$ vs. control

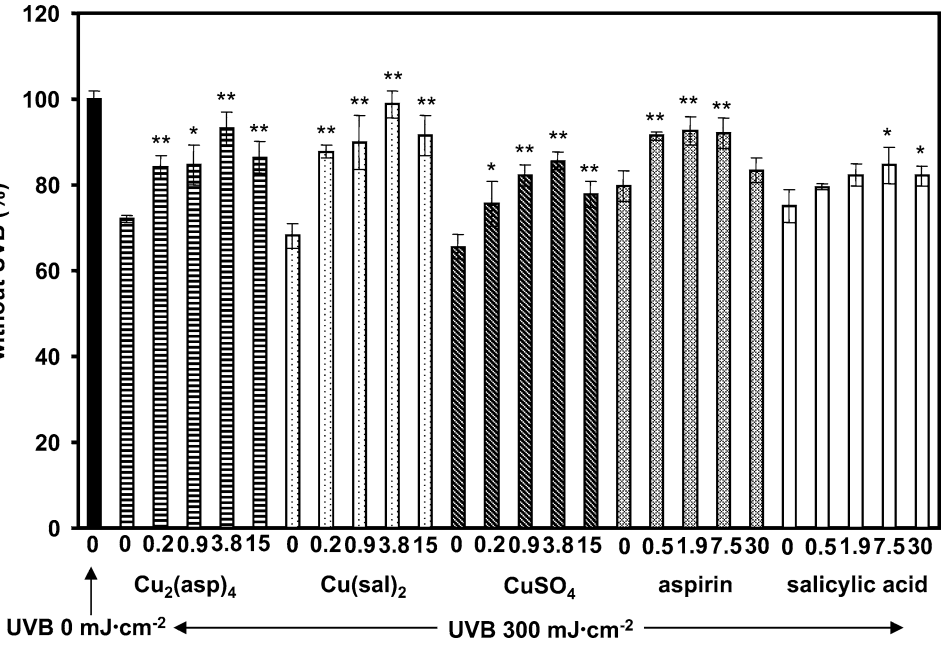

Fig. 5 Effects of $Cu_2(asp)_4$ and related compounds (in DMSO) on the survival of fibroblasts. Concentrations are in units of micrometers. The *left column* of each panel shows the control result without UVB irradiation. The other columns list results obtained for cells treated with complexes and UVB-irradiated. The indicated concentrations are based on Cu contents. Data are expressed as the mean ± SD for three replicate determinations. $^{**}P < 0.01$, $^{*}P < 0.05$ vs. control

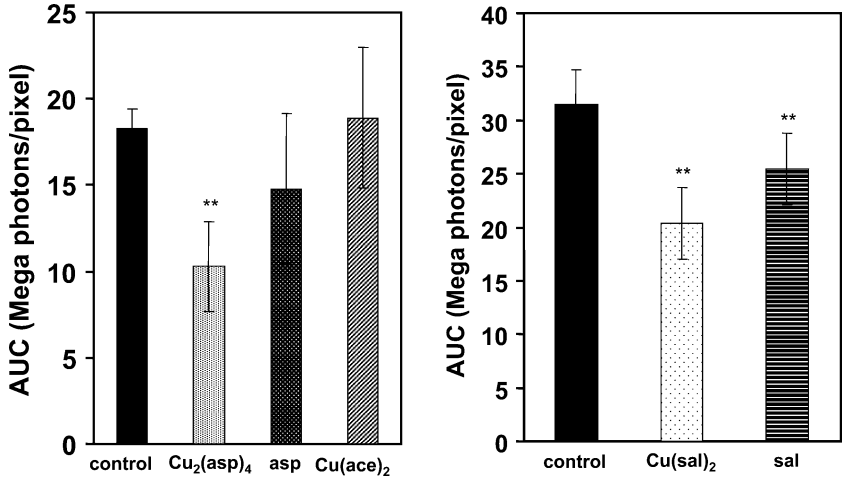

Fig. 6 Suppressive effects of $Cu_2(asp)_4$ and related compounds on UVA-induced ROS generation in the skin of HR-1 hairless mice treated orally for three consecutive days. Data are expressed as the mean ± SD for three or six mice. $^{**}P < 0.01$ vs. control

$Cu_2(asp)_4$ are occupied by neighboring acetyl oxygen atoms of $Cu_2(asp)_4$, whereas these positions are occupied by oxygen atoms of DMSO in the $Cu_2(asp)_4(DMSO)_2$ crystal. The coordination bonds of both complexes indicate that the average Cu–O bond length for the four equatorially coordinated oxygen atoms of these carboxylates, the Cu–O axially coordinated oxygen atom of DMSO or the neighboring acetyl group of $Cu_2(asp)_4$, and the Cu–Cu bond lengths are: 1.963(3), 2.131(3), and 2.632(1) Å, respectively, for $Cu_2(asp)_4(DMSO)_2$; 1.963(4), 2.241(8), and 2.617(3) Å, respectively, for $Cu_2(asp)_4$ with the axially bonded acetyl group of a neighboring molecule of $Cu_2(asp)_4$ [21]; and 1.953(12), (and 1.971(11) Å for the second molecule of DMF), 2.154(12) Å, and 2.615(4) Å, respectively, for the $Cu_2(asp)_4(DMF)_2$ solvate [36] (Table 3). The coordination bond length at the axial position is significantly shorter in $Cu_2(asp)_4(DMSO)_2$ than in $Cu_2(asp)_4(DMF)_2$, while the Cu–Cu bond length is longer in $Cu_2(asp)_4(DMSO)_2$ than the others, which may be due to the greater nucleophilicity of DMSO. This difference is also reflected in the magnetic susceptibilities of these compounds (Table 1).

Table 5 Suppression of reactive oxygen species generation with UVA irradiation of HR-1 hairless mouse skin after oral treatment for three consecutive days

Treatment	% Suppression vs. control
$Cu_2(asp)_4$	44
$Cu(sal)_2$	35
Aspirin	17
Salicylic acid	19
$Cu(ace)_2$	0

The ESR spectra showed that $Cu_2(asp)_4$ exists only in the mononuclear state, $Cu(asp)_2$, in this polar solvent, as

Table 6 Cu concentration in the blood and skin of ICR mice treated with Cu compounds or ligands

Compound	Concentration of Cu		
	Blood (μg/ml)		Skin (μg/g)
	30 min	90 min	90 min
Control	1.15 ± 0.06	1.15 ± 0.07	1.59 ± 0.19
$Cu_2(asp)_4$	1.22 ± 0.02	1.27 ± 0.08	1.70 ± 0.18
$Cu(sal)_2$	0.99 ± 0.04 **	1.24 ± 0.06	1.53 ± 0.20
$Cu(ace)_2$	1.50 ± 0.15 **	1.19 ± 0.17	1.63 ± 0.16
asp	0.94 ± 0.08 **	1.07 ± 0.04	1.55 ± 0.12
sal	0.96 ± 0.03 **	0.95 ± 0.01 **	1.54 ± 0.27

Δ= 0.07; Δ= 0.35; Δ= 0.12; Δ= 0.09; Δ= 0.04; Δ= 0.11; Δ= 0.04

** $P < 0.01$ *versus* control

indicated previously in other Cu(II) complexes [38]. Since the Cu atoms account for the antioxidative activity, the present results demonstrate that coordination structure of the metalloelement complex is important for biological activity [10].

Based upon results obtained for three different evaluation systems for $\cdot O_2^-$ scavenging activity (Table 4), the activities of these Cu(II) compounds were found to be essentially equivalent, which is attributed to the reactivities of mononuclear complexes in all cases. Although these activities are approximately only 1.6×10^{-3} times the reactivity of Cu_2Zn_2SOD, which has little or no activity when studied in test systems in vivo, small molecular mass complexes are effective in systems in vivo [8, 9] as well as in the xanthine/xanthine oxidase/cytochrome c and ESR in vitro systems. These results have confirmed and extended the existing literature [8, 9], and they are consistent with the SOD-mimetic reactivities of many small molecular mass copper complexes, including $Cu_2(asp)_4$ and $Cu(asp)_2$ complexes. Based upon the direct ESR measurement of SOD-mimetic reactivity (Fig. 3), we have further confirmed that Cu(II) compounds react with $\cdot O_2^-$ directly when scavenging $\cdot O_2^-$ and that the $Cu_2(asp)_4(DMSO)_2$ complex was the most active complex among the four different Cu(II) compounds.

Despite the relatively low SOD mimetic activity of $Cu_2(asp)_4$ and $Cu(sal)_2$ compared to Cu_2Zn_2SOD, such compounds have been confirmed as enhancing cell survival following UVB irradiation (Figs. 4, 5). At present, it is difficult to unequivocally explain cell survival in the presence of Cu(II) complexes following UVB irradiation; however, we speculate that Cu(II) compounds enter into cells and scavenge the generated ROS, or they induce several Cu-dependent antioxidative proteins or enzymes such as Cu_2Zn_2SOD, which is known to enhance cell survival following UV and ionizing irradiation injuries [10].

Encouraged by the enhancement of cell survival due to the presence of Cu(II) compounds, we examined the ROS suppressive effects of Cu(II) complexes in the skin of hairless mice following oral treatment. $Cu_2(asp)_4$ significantly suppressed ROS generation in the skin of UVA-irradiated mice more effectively than $Cu(sal)_2$ or control aspirin- or salicylic acid-treated mice, where Cu complexes of salicylic acid or aspirin may have formed in vivo [8] (Table 5; Fig. 6). Previously, we proposed that both superoxide and singlet oxygen ($^1O_2$) are formed during the exposure of the skin of live animals to UVA[31]. In the present study, it was observed that $Cu_2(asp)_4$ did not exhibit $^1O_2$ scavenging activity but did show $\cdot O_2^-$ scavenging activity (Table 4); therefore, the suppression of ROS generated in the UVA-exposed skin by the $Cu_2(asp)_4$ complex may be related to the scavenging of $\cdot O_2^-$ and the prevention of $^1O_2$ daughter product formation in the skin or perhaps the induction of some antioxidant enzymes including Cu_2Zn_2SOD [8] following Cu(II) incorporation into apoSOD (Zn_2SOD) in vivo.

Because a number of ROS-generating systems such as XOD and NADPH oxidase are localized within cells and on cell membranes [38], membrane lipids are actually susceptible to ROS attack. In terms of preventing lipid molecules from reactions with ROS, Fisher et al [11] developed lipophilic Cu(II) complexes that localize within lipid structures such as lipoproteins and cellular membranes. Measurement of the oil–water partition coefficient ($K = C_{\text{oleyl alcohol}}/C_{\text{water}}$) of $Cu_2(asp)_4$ showed that $Cu_2(asp)_4$ has oil-soluble characteristics, $K = 1.3$, i.e., log $P = 0.1$ [20]. This finding suggests that $Cu_2(asp)_4$ is a lipophilic complex, which can be transported to and localized in cell membranes and can scavenge $\cdot O_2^-$ there.

Available Cu concentrations in both blood and skin of mice treated orally on consecutive days with $Cu_2(asp)_4$ were found to be slightly increased, suggesting

that $Cu_2(asp)_4$ is distributed in tissue due to its lipophilic character.

In conclusion, it was observed that $Cu_2(asp)_4$ is a potent antioxidative compound and we have established its antioxidative activity in biological systems [8]. We propose here that $Cu_2(asp)_4$ is a potent antioxidative agent that could be used in the future to treat ROS-relevant diseases.

Acknowledgements We express our gratitude to Dr. H. Masaki, Mrs. M. Obayashi, and Ms. S. Yamada of the Cosmos Technical Center, Japan for their kind help and advice during the present study.

References

1. Towyz RM (2004) Hypertention 44(3):248–252
2. Petkau A (1986) Cancer Treat Rev 13:17–44
3. Mosaad AMA, Mohammad ME, Mohammad E, Mohsen R, Salah N (2003) Clin Chim Acta 337(1–2):23–33
4. Sorenson JRJ (1976) J Med Chem 19:135–148
5. Weser U, Richter C, Wendel A, Younes M (1978) Bioinorg Chem 8:201–213
6. Ohtsu H, Shimazaki Y, Odani A, Yamauchi O, Mori W, Itoh S, Fukuzumi S (2000) J Am Chem Soc 122:5733–5741
7. Cejudo-Marin R, Alzuet G, Ferrer S, Borras J, Castineiras A, Monzani E, Casella L (2004) Inorg Chem 43:6805–6814
8. Sorenson JRJ (1989) Prog Med Chem 26:437–568
9. Sorenson JRJ (1995) In: Berthon G (eds) Handbook of metal-ligand interactions in biological fluids: bioinorganic medicine, vol 2. Marcel Dekker, New York, pp 1128–1139
10. Sorenson JRJ (2002) Curr Med Chem 9:1867–1890
11. Fisher AEO, Grace L, Declan PN, (2005) Biochem Biophys Res Commun 329:930–933
12. Itami C, Matsunaga H, Sawada T, Sakurai H, Kimura Y (1993) Biochem Biophys Res Commun 197:536–541
13. Yamato K, Miyahara I, Ichimura A, Hirotsu K, Kojima Y, Sakurai H, Shiomi D, Sato K, Takui T (1999) Chem Lett 295–296
14. Jitsukawa K, Harata M, Arii H, Sakurai H, Masuda H (2001) Inorg Chim Acta 324:108–116
15. Lippard SJ, Burger RA, Ugurbil K, Pantoliano WM, Valentine SJ (1977) Biochemistry 16:1136–1141
16. Shen Z, Chen P, Li L, Chen P, Liu W (2004) Acta Pharmacol Sin 25:576–580
17. Tohgi H, Konno S, Tamura K, Kimura B, Kawano K (1992) Stroke 23:1400–1403
18. Bair BW, Hart N, Einspahr J, Liu G, Dong Z, Alberts D, Bowden TG (2002) Cancer Epidemiol Biomarkers Prev 11:1645–1652
19. Huang C, Ma W, Hanenberger D, Cleary M, Bowden TG, Dong Z (1997) J Biol Chem 272:26325–26331
20. Williams AD, Walz TD, Foye OW (1976) J Pharm Sci 65:126–128
21. Manojlovic-Muir L (1973) Acta Cryst B29:2033–2037
22. Walker RW, Beveridge JS, Whitehouse WM (1980) Agents Actions 10:38–47
23. Sheldrick GM (1997) SHELXS97. Program for the solution of crystal structure. University of Gottingen, Gottingen
24. Wilson AJC (ed) (1992) International tables for X-ray crystallography, vol C. Kluwer, Dordrecht
25. Sheldrick GM (1997) SHELXL97. Program for the refinement of crystal structures. University of Gottingen, Gottingen
26. Babior MB, Kipnes SR, Curnutte TJ (1973) J Clin Invest 52:741–744
27. Jinno J, Mori H, Oshiro Y, Kikuchi T, Sakurai H (1991) Free Rad Res Commun 15:223–230
28. Gao D, Kakuma M, Oka S, Sugiuo K, Sakurai H (2000) Bioorg Med Chem 8:2561–2569
29. Masaki H, Okano Y, Ochiai Y, Obayashi K, Akamatsu H, Sakurai H (2002) Free Rad Res 36:705–709
30. Masaki H, Sakurai H (1997) J Dermatol Sci 14:207–216
31. Masaki H, Sakurai H (1995) Photomed Photobiol 17:121–124
32. Yasui H, Sakurai H (2000) Biochem Biophys Res Commun 269:131–136
33. Yasui H, Sakurai H (2003) Exp Dermatol 12:655–661
34. Cozar O, David L, Chis V, Cosma C, Znamirovschi V, Damian G, Bratu I, Bora G (1995) Appl Magn Reson 8:235–242
35. Peisach J, Blumberg WE (1974) Arch Biochem Biophys 165:691–708
36. Viossat B, Daran J, Savouret G, Morgant G, Greenaway F, Dung N, Pham-Tran V, Sorenson JRJ (2003) J Inorg Biochem 96:375–385
37. Greenaway FT, Norris LJ, Sorenson JRJ (1988) Inorg Chim Acta 145:279–284
38. Kelley EE, Trostschansky A, Rubbo H, Freeman BA, Radi R, Tarpey MM (2004) J Biol Chem 279:37231–37234